Optimization of Radioimmunotherapy of Renal Cell Carcinoma: Labeling of Monoclonal Antibody cG250 with ^{131}I, ^{90}Y, ^{177}Lu, or ^{186}Re

Adrienne H. Brouwers, MD[1]; Julliëtte E.M. van Eerd, MSc[1]; Cathelijne Frielink, MSc[1]; Egbert Oosterwijk, PhD[2]; Wim J.G. Oyen, MD, PhD[1]; Frans H.M. Corstens, MD, PhD[1]; and Otto C. Boerman, PhD[1]

[1]*Department of Nuclear Medicine, University Medical Center Nijmegen, Nijmegen, The Netherlands; and* [2]*Department of Urology, University Medical Center Nijmegen, Nijmegen, The Netherlands*

Radioimmunotherapy (RIT) can be performed with various radionuclides. We tested the stability, biodistribution, and therapeutic efficacy of various radioimmunoconjugates (^{131}I, $^{88/90}$Y, ^{177}Lu, and ^{186}Re) of chimeric antirenal cell cancer monoclonal antibody G250 (mAb cG250) in nude mice with subcutaneous renal cell cancer (RCC) tumors. **Methods:** The $^{88/90}$Y and ^{177}Lu labeling procedures of cG250 conjugated with cyclic diethylenetriaminepentaacetic acid anhydride (cDTPA), isothiocyanatobenzyl-DTPA (SCN-Bz-DTPA), or 1,4,7,10-tetraazacyclododecanetetraacetic acid (DOTA) were characterized. Stability of the labeled conjugates in plasma at 37°C was assessed. Biodistribution and therapeutic efficacy of labeled cG250 were compared in nude mice with SK-RC-52 human RCC xenografts. **Results:** Both SCN-Bz-DTPA and DOTA were stable in vitro (<5% release of the radiolabel during 14 and 21 d of incubation) and in vivo (uptake in bone ≤ 1.5 percentage injected dose per gram [%ID/g] at 7 d after injection) when used to label ^{88}Y or ^{177}Lu to cG250. The DOTA conjugate was slightly but significantly more stable than SCN-Bz-DTPA at 7 d after injection. In vivo, these cG250 preparations showed high tumor uptake (70 ± 15 %ID/g ± SD at 7 d after injection). Maximum tumor uptake for ^{125}I-cG250 and ^{186}Re-mercaptoacetyltriglycine-(MAG3)-cG250 (<20 ± 3 %ID/g ± SD) was reached at 3 d after injection and was much lower in comparison with cG250 labeled with the residualizing radionuclides. Because the highest specific activities could be prepared using SCN-Bz-DTPA, and relatively low protein doses of cG250 could be administered without saturating the tumor, cG250-SCN-Bz-DTPA conjugates were used in RIT studies. In RIT experiments at maximum tolerated dose, tumor growth was delayed most effectively by cG250 labeled with ^{177}Lu, next most effectively by ^{90}Y and ^{186}Re (which were approximately equal), and least by ^{131}I (delayed by approximately 185, 125, 90, and 25 d, respectively). The best median survival (300 d) was observed for ^{177}Lu-SCN-Bz-DTPA-cG250. Median survival for control groups was <150 d. **Conclusion:** DOTA-conjugated radiolabeled antibodies were the most stable radioimmunoconjugates in vitro and in vivo as manifested by the lowest bone uptake. However, specific activity was higher for SCN-Bz-DTPA. The RIT studies clearly showed that the therapeutic efficacy of mAb cG250 labeled with ^{177}Lu, ^{90}Y, or ^{186}Re was superior to that of ^{131}I-cG250. The residualizing radionuclides ^{177}Lu and ^{90}Y led to higher radiation doses to the tumor and most likely are better candidates than conventionally radiolabeled ^{131}I for RIT with cG250 in patients with RCC.

Key Words: renal cell carcinoma; monoclonal antibody cG250; experimental radioimmunotherapy; radionuclides; chelates

J Nucl Med 2004; 45:327–337

The goal of this investigation was to develop an effective radioimmunotherapy (RIT) approach for metastasized renal cell carcinoma (RCC) using the chimeric (c) monoclonal antibody (mAb) G250. Until now, mAb cG250 has been labeled with ^{131}I for RIT (*1*,*2*). Radioiodination of mAbs is relatively easy to perform, and ^{131}I is widely available and relatively inexpensive. However, ^{131}I is not an optimal radionuclide for RIT, since this radionuclide is readily released from the tumor after internalization of the mAbs and has an abundance of high-energy γ-photons (Table 1), which is a concern for radiation safety.

Residualizing radionuclides, such as ^{90}Y and ^{177}Lu, are potentially more suitable radionuclides for RIT (Table 1). The 11-mm tissue penetration range of the β-emissions of ^{90}Y is much higher than the comparable 3-mm range of ^{131}I. Apart from some bremstrahlung, ^{90}Y does not emit γ-photons, so there is less need for patient shielding after high-dose treatment. The limitation of ^{90}Y is the inability to scintigraphically visualize the distribution of the therapeutic dose throughout the body. The 2-mm range of the β-particles of ^{177}Lu is of the same order as the range of ^{131}I β-particles. The physical characteristics of ^{177}Lu γ-photons (208 keV, 11% abundancy) are ideal for imaging and also from a radiation safety point of view. Because of the range of β-particles, ^{90}Y seems particularly well suited for the treatment of relatively large solid tumor masses, and ^{177}Lu may have an advantage in treating small lesions (*3*).

Received Jul. 7, 2003; revision accepted Oct. 14, 2003.

For correspondence or reprints contact: Otto C. Boerman, PhD, Department of Nuclear Medicine, UMC Nijmegen, P.O. Box 9101, NL-6500 HB Nijmegen, The Netherlands.

E-mail: o.boerman@nucmed.umcn.nl

TABLE 1
Characteristics of Radionuclides

Radionuclide	Half-life (days)	β-Radiation		γ-Radiation	
		E_{max} (MeV)	Abundancy	keV	Abundancy
^{131}I	8	0.6	89%	364	81%
^{90}Y	2.7	2.28	100%		
^{177}Lu	6.7	0.5	79%	208	11%
		0.18	12%	113	6%
^{186}Re	3.8	1.08	71%	137	9%
		0.9	22%		

When released from the antibody, the metallic radionuclides ^{90}Y and ^{177}Lu are partly incorporated into the mineral bone (*4*), which may lead to excessive radiation to the bone marrow (*5*). To prevent in vivo dissociation of ^{90}Y and ^{177}Lu from the antibody, various chelates have been developed and tested both in vitro and in vivo. Initially, cyclic anhydride diethylenetriaminepentaacetic acid (cDTPA) was used to label mAbs with ^{90}Y, because this chelate formed very stable complexes with ^{111}In (*6*). However, mAbs labeled with ^{90}Y via this chelate were unstable, leading to excessive accumulation of released ^{90}Y in the bone (*5,7*). Therefore, bifunctional chelates based on DTPA (e.g., isothiocyanatobenzyl-DTPA [SCN-Bz-DTPA] and macrocyclic chelates such as 1,4,7,10-tetraazacyclododecanetetraacetic acid [DOTA]) were developed for mAb-labeling purposes (*7–10*).

In addition to high stability and retained immunoreactivity after radiolabeling, the specific activity that can be obtained is also important in selecting a suitable chelate, especially in RIT of RCC with cG250. The most optimal protein dose for tumor targeting with cG250 is relatively low compared with other mAb-antigen systems. We have shown in patients with RCC that high uptake in the tumor (expressed as percentage injected dose per gram [%ID/g]) could be obtained only if the total cG250 protein dose per patient did not exceed 10 mg (*1*). For ^{90}Y- or ^{177}Lu-labeled antibodies in RIT in humans, one would aim to administer an activity dose of 1,110–2,220 MBq (30–60 mCi) ^{90}Y or 5,550–7,400 MBq (150–200 mCi) ^{177}Lu. This implies that for a protein dose of 5–10 mg, a specific activity $>$ 370 MBq/mg ($>$10 mCi/mg) is a prerequisite for RIT with cG250 in patients with RCC.

Another radionuclide that has become available for RIT is ^{186}Re, with a β-particle range of 5 mm (Table 1). It has chemical properties similar to those of ^{99m}Tc, and the energy of the emitted γ-photons is similar as well. ^{186}Re is therefore well suited for imaging with a γ-camera. As with ^{177}Lu, the limited percentage of γ-emissions (9%) of ^{186}Re provides a major advantage from a radiation safety point of view, and the in vivo distribution of a therapeutic dose of ^{186}Re-labeled antibody can be imaged scintigraphically. Several ^{186}Re mAb-labeling methods have been described. The direct labeling method described by Griffiths et al. (*11*) results in low ^{186}Re-to-mAb molar ratios, and the ^{186}Re–mAb complex is unstable in vivo. The indirect labeling method described by Fritzberg et al. (*12*) and optimized by Visser et al. (*13*) using mercaptoacetyltriglycine (MAG3) as a chelate yielded relatively high ^{186}Re-MAG3–to–mAb molar ratios, resulting in higher specific activities, and is suitable for RIT purposes. The β-emitter ^{188}Re is less suited for RIT with IgG mAbs. The physical half-life (17 h) does not match with the relatively slow pharmacokinetics and tumor accretion of cG250 IgG (*1*).

To determine the most optimal radioimmunoconjugate to be labeled with mAb cG250 for RIT in humans, a series of experiments was designed. First, the in vitro and in vivo characteristics of cG250 labeled with ^{90}Y and ^{177}Lu using 3 different chelates (cDTPA, SCN-Bz-DTPA, and DOTA) were directly compared. The labeling efficiency, in vitro stability, and immunoreactivity of each of the labeled immunoconjugates were determined. Subsequently, the biodistribution of these radioimmunoconjugates was studied and compared with the biodistribution of ^{125}I-cG250 and ^{186}Re-MAG3-cG250 in nude mice with subcutaneous SK-RC-52 human RCC xenografts. Finally, the therapeutic efficacies of maximum tolerable activity doses (MTDs) of ^{90}Y-SCN-Bz-DTPA-cG250, ^{177}Lu-SCN-Bz-DTPA-cG250, ^{131}I-cG250, and ^{186}Re-MAG3-cG250 were studied.

MATERIALS AND METHODS

Monoclonal Antibody cG250

The isolation and immunohistochemical reactivity of mAb G250 have been described elsewhere (*1,14*). To reduce the immunogenicity of the antibody, a chimeric version has been developed (*15*). MAb cG250 is reactive with the antigen G250 ($K_a = 4 \times 10^9$ L/mol), which has been identified as the tumor-associated isoenzyme carbonic anhydrase isoenzyme IX (MN/CA IX) (*16*). It is expressed on the cell surface of nearly all clear-cell RCCs and is absent on most other normal tissues and malignancies (*1,14,17,18*). The majority of RCCs (75%) are of the clear-cell type (*14,16*).

Conjugation, Radiolabeling, and Quality Control

The conjugation of cDTPA (Fig. 1A) (Sigma) and SCN-Bz-DTPA (Fig. 1B) (Macrocyclics) to mAb cG250 was performed in a 0.1-mol/L $NaHCO_3$ buffer with pH 8.2 and using a 100-(cDTPA) or 50-fold (SCN-Bz-DTPA) molar excess, as described by Ruegg et al. (*19*) with minor modifications (conjugation period

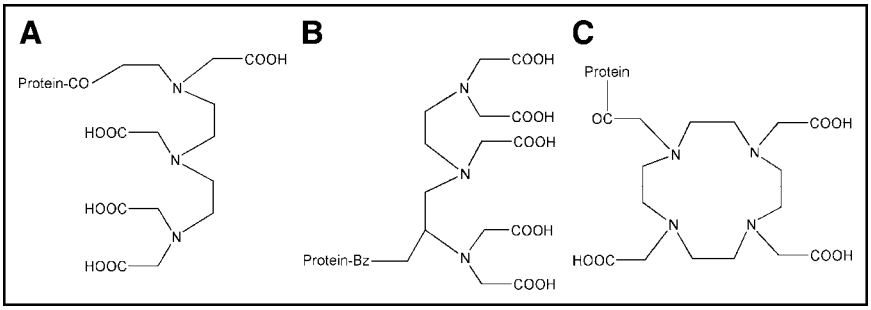

FIGURE 1. Structure of the ligands used: cDTPA (A), SCN-Bz-DTPA (B), and DOTA (C).

of 1 h at room temperature). cDTPA served as a reference for the 2 other immunoconjugates used (SCN-Bz-DTPA-cG250 and DOTA-cG250), because it is known that conjugation of cDTPA to mAbs leads to unstable radioimmunoconjugates when labeled with ^{90}Y or ^{177}Lu. The cDTPA-cG250 and SCN-Bz-DTPA-cG250 conjugates were labeled with either ^{88}Y (Isotope Products Europe Blaseg) or ^{90}Y (Perkin Elmer) or ^{177}Lu (University of Missouri Research Reactor) in a 0.1 mol/L ammonium acetate buffer of pH 5.4 for 30 min at room temperature. For the in vitro stability tests and biodistribution experiments, the γ-emitter ^{88}Y was substituted for ^{90}Y. Similarly, ^{125}I was used instead of ^{131}I in the biodistribution experiments.

The activation and conjugation of DOTA (Fig. 1C) was performed as described by Lewis et al. (*20*). The DOTA-cG250 conjugate was labeled with either $^{88/90}$Y or ^{177}Lu in an ammonium acetate buffer with pH 5.4 for 60 min at 45°C. The number of DTPA or DOTA ligands per cG250 molecule was determined as described by Hnatowich et al. (*6*).

MAb cG250 was radioiodinated with ^{125}I (Amersham) and ^{131}I (MDS Nordion) according to the IODO-GEN method (Pierce) (*1*,*21*). The labeling of the MAG3 chelate with ^{186}Re (Mallinckrodt) and the conjugation of the radioactive chelate to mAb cG250 were performed essentially as described by Visser et al. (*12*).

All conjugation and labeling procedures using ^{177}Lu or $^{88/90}$Y were performed under strict metal-free conditions. All radiolabeled cG250 preparations were purified by gel filtration on a PD-10 column (Amersham Pharmacia Biotech) and eluted with phosphate-buffered saline (PBS) supplemented with 0.5% bovine serum albumin (BSA). For all preparations, the amount of non–mAb-bound radiolabel was determined by instant thin-layer chromatography (ITLC) using ITLC silica gel strips (Gelman Sciences, Inc.), using 0.1 mol/L citrate buffer (pH 6.0) as the mobile phase ($R_f = 0$ for radioimmunoconjugates, and $R_f = 0.8–1$ for free and chelated radionuclides).

The immunoreactive fraction at infinitive antigen excess of all radiolabeled cG250 preparations was determined on freshly trypsinized SK-RC-52 RCC cells essentially as described by Lindmo et al. (*22*), with minor modifications (*1*).

In Vitro Stability

The stabilities of the various ^{88}Y- and ^{177}Lu-labeled preparations were assessed in vitro by diluting in plasma at an activity concentration of 18.5 kBq/mL (0.5 μCi/mL) for the ^{88}Y preparations and 1,850 kBq/mL (50 μCi/mL) for the ^{177}Lu preparations. A final concentration of 0.5 mmol/L ethylenediaminetetraacetic acid (EDTA) was added to capture released radiometal, and the preparations were incubated at 37°C. Plasma samples were analyzed at 0 and 4 h and at 1, 2, 5, 7, 9, 12, 15, 19, and 22 d by fast protein liquid chromatography (FPLC) using a Biosep Sec-S3000 gel filtration column (Phenomenex). In a previous study, we demonstrated that ^{131}I-cG250 and ^{186}Re-MAG3-cG250 were stable (<5% release of the radiolabel) in plasma up to 30 h using the same method (*21*).

Nude Mouse Tumor Model

The RCC cell line SK-RC-52 was derived from a mediastinal metastasis of a primary RCC and has been described elsewhere (*23*). SK-RC-52 cells were cultured in RPMI medium (Life Technologies) supplemented with 10% fetal calf serum (FCS) at 37°C in a humidified atmosphere with 5% CO_2. Cells were washed in saline, trypsinized, and washed in RPMI + 10% FCS, and 2×10^6 cells (in 0.2 mL of RPMI medium) were injected subcutaneously into the right flank of 6- to 8-wk-old BALB/c *nu/nu* mice. Biodistribution and RIT experiments were initiated 14–16 d after inoculation of tumor cells. All animal experiments were approved by the Animal Experiments Committee of the University Medical Center Nijmegen and performed in accordance with its guidelines.

Biodistribution Experiments

To study the biodistribution of the various ^{88}Y-labeled immunoconjugates, RCC-tumor-bearing mice (median tumor weight, 0.08 g) were divided randomly into groups of 15 mice. Mice were injected intravenously with 37 kBq (1 μCi) ^{88}Y-cDTPA-cG250 or ^{88}Y-SCN-Bz-DTPA or 22.2 kBq (0.6 μCi) ^{88}Y-DOTA-cG250, each diluted in PBS + 0.5% BSA. In a similar experiment, mice were injected intravenously with 185 kBq (5 μCi) ^{177}Lu-cDTPA-cG250, ^{177}Lu-SCN-Bz-DTPA-cG250, or ^{177}Lu-DOTA-cG250. Also, 2 groups of 15 mice were injected intravenously with 185 kBq (5 μCi) ^{125}I-cG250 or 1,850 kBq (50 μCi) ^{186}Re-MAG3-cG250. All mice received a protein dose of 25–50 μg cG250 (volume, 200 μL/mouse). In each group, 5 mice were killed at 1, 3, or 7 d after injection, and the biodistribution of the radiolabel was determined. The tumor and normal tissues (blood, muscle, femur without marrow, lung, spleen, kidney, liver, and small intestines without contents) were dissected, weighed, and counted in a γ-counter (Wizard; Pharmacia-LKB). To correct for radioactive decay, injection standards were counted simultaneously. The activity in samples was expressed as %ID/g tissue.

Maximum Tolerated Dose

The MTD of every radiolabeled cG250 preparation in mice was determined. BALB/c *nu/nu* mice (6–8 wk old, 5 per group) were injected intravenously with escalating doses of ^{131}I-cG250 (7.4, 11.1, 14.8, 18.5, or 22.2 MBq [200, 300, 400, 500, or 600 μCi]), ^{90}Y-SCN-Bz-DTPA-cG250 (2.8, 3.7, 4.6, 5.6, 6.5, 7.4, or 11.1 MBq [75, 100, 125, 150, 175, 200, or 300 μCi]), or ^{177}Lu-SCN-Bz-DTPA-cG250 (19.4, 22.2, 25.9, or 29.6 MBq [525, 600, 700, or 800 μCi]). The MTD for ^{186}Re-MAG3-cG250 was derived from

similar experiments obtained with another intact IgG mAb used simultaneously at our department (9.3, 13.0, 18.5, or 24.1 MBq [250, 350, 500, or 650 μCi]). After injection, the mice were weighed and survival was monitored twice weekly during 2 mo. MTD was set 1 dose level below the dose level leading to >20% decrease in total body weight in at least 1 of the mice or early death of at least 1 mouse.

Dosimetry

Radiation dose estimates to the tumors of mice in the RIT experiments were determined by integrating the trapezoidal regions defined by the time–activity data from the biodistribution experiments. The resulting integral was converted to mGy/MBq using S values (MIRDOSE3; unit density sphere model) appropriate for each radionuclide and assuming a tumor weight of 0.055 g, corresponding approximately to the mean tumor volume at the start of the RIT experiments (51 mm^3) (*24*). Mean absorbed dose in the tumor was further calculated by multiplying by the respective MTD of each radiolabeled cG250 preparation. Absorbed dose in the tumor was calculated for ^{90}Y using the ^{88}Y biodistribution data and for ^{131}I using the ^{125}I biodistribution data.

Radioimmunotherapy Experiments

Based on the results of the radiolabeling and biodistribution studies, SCN-Bz-DTPA was selected instead of DOTA as a chelate for labeling ^{90}Y and ^{177}Lu to cG250 in subsequent RIT experiments. High specific activities, a necessity for RIT experiments with cG250 in humans, could be obtained with SCN-Bz-DTPA, and biodistribution experiments in mice showed only a slight advantage for the DOTA conjugates.

RIT studies were performed on nude mice (10 per group) with small (mean volume, 51 ± 35 mm^3) subcutaneous SK-RC-52 tumors. Mice received cG250 labeled with ^{131}I, ^{90}Y-SCN-Bz-DTPA, ^{177}Lu-SCN-Bz-DTPA, or ^{186}Re-MAG3 intravenously at MTD (protein doses of 30, 30, 60, and 35 μg per mouse, respectively). Mice in control groups received unlabeled cG250, PBS, or 5.6 MBq (150 μCi) ^{90}Y-SCN-Bz-DTPA-cU36, the last serving as an irrelevant control mAb in this study (protein dose of 30 μg per mouse for the 2 cG250 groups) (*25*). In this tumor model, a cG250 antibody protein dose ≤ 60 μg was used to avoid a decrease of tumor uptake at higher protein doses as a result of saturation of accessible antigens in the tumor. In separate biodistribution studies in nude mice with subcutaneous SK-RC-52 tumors injected with variable protein doses of cG250 (3, 10, 30, 60, 90, 100, or 300 μg), only at protein doses ≥ 90 μg was cG250 uptake in RCC tumors decreased (unpublished data, 2003).

Tumor size was measured in 3 dimensions twice weekly with a caliper for the first 100 d and once each week thereafter. Tumor volume was calculated as:

$$\text{Volume} = 4/3 \times \pi \times r_1 \times r_2 \times r_3,$$

where r is tumor radius, expressed in cubic millimeters. When tumor volume exceeded 2 cm^3, mice were killed for humane reasons. Survival curves according to the Kaplan–Meier method were generated for each group. Mean tumor growth over time per group was calculated and expressed as relative tumor growth: tumor volume (V) divided by tumor volume at day 0 (V_0). When a mouse died or was killed during the experiment, its last observed tumor volume was used to calculate the mean tumor growth curve in the corresponding group. The delay in exponential tumor growth (expressed in days) for each mouse was determined as follows. If tumor volume increased without a temporary delay in the individual tumor growth curve after injection of one of the preparations, then tumor growth delay was set at 0 d. This was the case in most mice in the control groups (unlabeled cG250, PBS, and ^{90}Y-cU36). In the groups that received radiolabeled cG250, most often a temporary maximum tumor volume was reached in the first 50 d after injection, expressed as V_1max on day d_1. In subsequent days, the tumor volume decreased, after which the tumor volume increased again. The day on which V_1max was reached for the second time was determined and designated as day d_2. The delay in exponential tumor growth was defined as and calculated by subtracting d_1 from d_2. For each group, mean and SD of exponential tumor growth delay were calculated.

Statistical Analysis

Statistical analysis of bone uptake in the biodistribution experiments was performed using Bonferroni-corrected, repeated-measures, 1-way ANOVA. The software package SPSS version 10.0 (SPSS Inc.) was used for statistical analysis of the RIT experiments. Because of lack of homogeneity of variances, the nonparametric procedure of Kruskal–Wallis was applied to look for significant differences in exponential tumor growth delay between the groups. Kaplan–Meier survival curves were analyzed for differences using the log-rank test. Differences were considered significant when $P < 0.05$ (2-sided).

RESULTS

Conjugation, Radiolabeling, and Quality Control

From 1 to 3 DTPA/DOTA moieties were conjugated per IgG molecule. Table 2 shows the maximum specific activity that could be obtained with each of the immunoconjugates. The maximum specific activity of the DOTA radioimmunoconjugates was approximately half the value that could be obtained with the cDTPA-cG250 and SCN-Bz-DTPA-cG250 conjugates. The radiochemical purity after PD-10 purification was always >95%, except for the cDTPA radioimmunoconjugates (Table 2). All preparations retained their immunoreactivity (Table 2).

Approximately 2 MAG3 moieties were conjugated per cG250 molecule. A specific activity of 518 kBq/μg (14 μCi/μg) was obtained for ^{186}Re-MAG3-cG250 and 370 kBq/μg (10 μCi/μg) for ^{131}I-cG250. The immunoreactivity immediately after labeling was ≥95% for both ^{131}I-cG250 and ^{186}Re-MAG3-cG250 (Table 2).

In Vitro Stability

FPLC analysis of the preparations after incubation in human plasma indicated that all DOTA and SCN-Bz-DTPA preparations were quite stable, because <5% of the radiolabel was released during 14 d of incubation (Fig. 2). ^{88}Y-DOTA-cG250 and ^{177}Lu-DOTA-cG250 were even more stable, showing <5% release during the complete incubation period (22 d) (Fig. 2). As expected, both cDTPA preparations were unstable in vitro, showing >10% release of the radiolabel in the first 24 h (Fig. 2).

Biodistribution Experiments

Biodistribution studies in nude mice with subcutaneous SK-RC-52 tumors showed relatively low blood levels for the ^{88}Y-cDTPA-cG250 preparation when compared with

TABLE 2
Characteristics of Radiolabeled Immunoconjugates

Preparation	Maximum specific activity in kBq/μg (μCi/μg)	Labeling efficiency (%)	RCP after purification (%)	Immunoreactivity (%)
^{90}Y-cDTPA-cG250	370 (10)	13	86	ND
^{90}Y-SCN-Bz-DTPA-cG250	370 (10)	90	98	100
^{90}Y-DOTA-cG250	111 (3)	94	98	80
^{177}Lu-cDTPA-cG250	296 (8)	15	75	89
^{177}Lu-SCN-Bz-DTPA-cG250	296 (8)	97	98	82
^{177}Lu-DOTA-cG250	111 (3)	94	99	87
^{131}I-cG250	1,850 (50)	87	98	96
^{186}Re-MAG3-cG250	307 (8)	43	99	95

RCP = radiochemical purity; ND = not determined.

^{88}Y-SCN-Bz-DTPA-cG250 and ^{88}Y-DOTA-cG250, as a result of the known instability of the former preparation (blood levels of 1.5 %ID/g versus 8.4 %ID/g and 8.2 %ID/g at 7 d after injection, respectively) (Table 3). Conversely, bone uptake was much higher for ^{88}Y-cDTPA–labeled cG250 than for ^{88}Y-SCN-Bz-DTPA-cG250 and ^{88}Y-DOTA-cG250 (10.7 ± 2.4 %ID/g versus 1.2 ± 0.2 %ID/g and 0.4 ± 0.3 %ID/g at 7 d after injection, respectively) (Table 3). Although femur uptake was low for both ^{88}Y-SCN-Bz-DTPA-cG250 and ^{88}Y-DOTA-cG250, indicating high stability of both radioimmunoconjugates, the difference became significant at 7 d after injection ($P = 0.05$). Both the ^{88}Y-SCN-Bz-DTPA– and the ^{88}Y-DOTA–labeled cG250 preparation showed high uptake in tumor (52 ± 7 %ID/g and 44 ± 15 %ID/g at 3 d after injection, with a further increase to 71 ± 8 %ID/g and 55 ± 11 %ID/g at 7 d after injection) (Fig. 3; Table 3). Uptake in other tissues at 7 d after injection was low and very similar for ^{88}Y-SCN-Bz-DTPA-cG250 and ^{88}Y-DOTA-cG250. The results of the ^{177}Lu-labeled cG250 preparations were comparable with those obtained with the ^{88}Y-labeled cG250 preparations. The difference in bone uptake between ^{177}Lu-SCN-DTPA-cG250 and ^{177}Lu-DOTA-cG250 was significant at all 3 time points ($P < 0.001$). Tumor uptake of ^{177}Lu-SCN-Bz-DTPA and ^{177}Lu-DOTA-cG250 was not significantly higher compared with groups that received the corresponding ^{88}Y-labeled cG250 immunoconjugates at 7 d after injection. However, uptake of ^{177}Lu-SCN-Bz-DTPA-cG250 generally was higher in normal tissues than was uptake of ^{177}Lu-DOTA-cG250 and significantly higher in spleen and liver at 3 and 7 d after injection ($P < 0.0001$). This phenomenon was not observed in the cG250 immunoconjugates labeled with ^{88}Y (Table 3).

In contrast, uptake of ^{125}I-cG250 was much lower in all tissues, especially in tumor (maximally 14 ± 3 %ID/g at 3 d after injection), whereas blood levels were similar compared with ^{88}Y/^{177}Lu-SCN-Bz-DTPA/DOTA-cG250, indicating a washout of the radioiodine label from the tumor (Table 3; Fig. 3). The biodistributions of ^{186}Re-MAG3-cG250 and ^{125}I-cG250 were nearly identical (Table 3; Fig. 3).

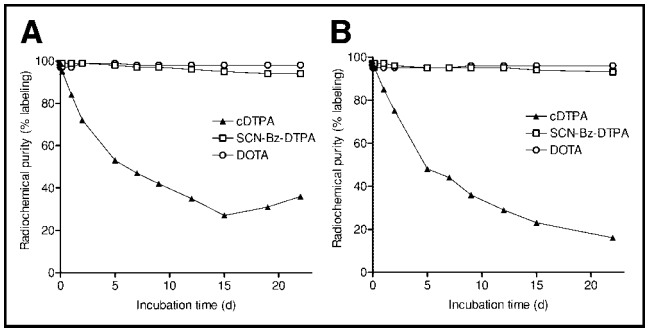

FIGURE 2. In vitro stability analyses using fast protein liquid chromotography for ^{88}Y-X-cG250 (A) and ^{177}Lu-X-cG250 (B) conjugated with 1 of 3 chelates: cDTPA, SCN-Bz-DTPA, or DOTA.

Dosimetry

For the various preparations, mean absorbed doses in the tumors at MTD were estimated as 76 Gy for ^{131}I-cG250, 95 Gy for ^{90}Y-SCN-Bz-DTPA-cG250, 104 Gy for ^{186}Re-MAG3-cG250, and 807 Gy for ^{177}Lu-SCN-Bz-DTPA-cG250 (Table 4).

Radioimmunotherapy Experiments

The MTDs of the various labeled cG250 preparations were 11.1 MBq (300 μCi) for ^{131}I-cG250, 5.6 MBq (150 μCi) for ^{90}Y-SCN-Bz-DTPA-cG250, and 18.5 MBq (500 μCi) for both ^{177}Lu-SCN-Bz-DTPA-cG250 and ^{186}Re-MAG3-cG250. Within 10 d after intravenous injection of the various preparations at MTD, 2 mice died unexpectedly: one in the ^{177}Lu group and another in the PBS control group. These deaths were not considered related to the injections, and these 2 mice were excluded from analysis. The survival curves (Fig. 4) show that the median survivals of the groups that received ^{177}Lu-SCN-Bz-DTPA, ^{90}Y-SCN-Bz-DTPA-cG250, ^{186}Re-MAG3-cG250, and ^{131}I-cG250 were significantly longer (294, 241, 211 and 164 d, respectively) than those of the unlabeled cG250, PBS, and ^{90}Y-cU36 control groups (range, 83–143 d) ($P < 0.001$).

TABLE 3
Biodistribution of Radiolabeled cG250 Immunoconjugates*

Organ	Days after injection†	Preparation							
		^{88}Y-cDTPA	^{88}Y-SCN-Bz-DTPA	^{88}Y-DOTA	^{177}Lu-cDTPA	^{177}Lu-SCN-Bz-DTPA	^{177}Lu-DOTA	^{125}I	^{186}Re-MAG3
Tumor	1	32.9 ± 7.2	34.8 ± 8.5	36.2 ± 14.1	34.6 ± 10.8	53.2 ± 21.1	41.3 ± 9.9	11.7 ± 1.5	13.5 ± 1.8
	3	46.6 ± 19.7	51.9 ± 7.0	44.4 ± 14.8	59.0 ± 11.5	113.3 ± 24.7	86.9 ± 14.5	14.0 ± 3.0	16.9 ± 2.8
	7	27.4 ± 4.8	70.9 ± 8.4	55.3 ± 10.7	45.0 ± 30.0	87.3 ± 14.0	74.5 ± 10.5	9.1 ± 2.0	7.9 ± 2.0
Muscle	1	0.8 ± 0.1	1.3 ± 0.4	1.3 ± 0.2	1.1 ± 0.3	1.4 ± 0.1	1.2 ± 0.2	1.4 ± 0.1	1.2 ± 0.4
	3	0.5 ± 0.1	1.2 ± 0.2	1.4 ± 0.2	0.6 ± 0.2	1.1 ± 0.2	1.1 ± 0.1	1.0 ± 0.1	1.1 ± 0.3
	7	0.2 ± 0.1	0.9 ± 0.3	0.7 ± 0.2	0.3 ± 0.1	0.6 ± 0.2	0.6 ± 0.1	0.6 ± 0.2	0.5 ± 0.2
Blood	1	12.8 ± 0.9	16.4 ± 2.3	15.2 ± 3.2	16.5 ± 1.4	21.0 ± 1.4	14.9 ± 1.2	16.9 ± 0.9	17.3 ± 1.4
	3	5.9 ± 0.8	11.8 ± 2.9	12.5 ± 1.3	6.7 ± 0.5	13.4 ± 3.8	11.3 ± 1.2	12.4 ± 1.3	14.8 ± 1.5
	7	1.5 ± 0.2	8.4 ± 1.8	8.2 ± 1.9	1.6 ± 1.0	5.9 ± 1.7	6.0 ± 1.6	6.8 ± 1.6	6.7 ± 1.0
Femur	1	6.3 ± 1.1	1.1 ± 0.5	0.7 ± 0.2	5.2 ± 1.2	1.3 ± 0.3	0.6 ± 0.2	0.7 ± 0.1	0.5 ± 0.2
	3	10.7 ± 1.3	1.3 ± 0.6	1.0 ± 0.2	11.0 ± 2.7	1.3 ± 0.3	0.2 ± 0.1	0.5 ± 0.0	0.4 ± 0.1
	7	10.7 ± 2.4	1.2 ± 0.2	0.4 ± 0.3	14.2 ± 4.7	1.5 ± 0.3	0.3 ± 0.2	0.4 ± 0.2	0.2 ± 0.1
Spleen	1	3.7 ± 0.6	3.4 ± 0.6	2.7 ± 0.4	5.2 ± 2.0	5.5 ± 0.9	3.4 ± 0.5	2.9 ± 0.2	2.7 ± 0.4
	3	3.4 ± 0.9	2.9 ± 0.6	2.8 ± 0.3	4.2 ± 0.8	6.3 ± 1.5	3.2 ± 0.5	2.1 ± 0.4	2.6 ± 0.4
	7	2.5 ± 0.5	3.0 ± 0.4	2.4 ± 0.3	4.8 ± 2.1	6.6 ± 2.1	2.9 ± 0.2	1.2 ± 0.3	1.0 ± 0.1
Kidney	1	7.1 ± 0.6	4.8 ± 0.6	4.8 ± 0.8	7.7 ± 0.5	6.7 ± 0.5	4.7 ± 0.4	4.4 ± 0.3	4.5 ± 0.2
	3	5.8 ± 0.7	3.9 ± 0.7	4.5 ± 0.5	6.1 ± 0.9	4.1 ± 1.3	3.8 ± 0.4	3.2 ± 0.3	3.6 ± 0.3
	7	3.9 ± 0.8	2.6 ± 0.4	2.7 ± 0.6	3.7 ± 0.9	2.4 ± 0.3	2.2 ± 0.4	1.8 ± 0.5	1.7 ± 0.3
Liver	1	6.5 ± 0.7	5.8 ± 0.9	5.7 ± 0.6	9.0 ± 0.5	10.4 ± 3.2	4.5 ± 0.4	3.7 ± 0.1	4.8 ± 0.5
	3	5.3 ± 0.2	5.9 ± 0.3	7.0 ± 0.7	10.1 ± 3.1	16.6 ± 5.6	4.2 ± 0.4	2.8 ± 0.1	3.5 ± 0.4
	7	4.9 ± 1.2	4.2 ± 0.6	3.7 ± 0.4	8.6 ± 2.1	16.7 ± 2.1	4.0 ± 0.6	1.7 ± 0.5	1.6 ± 0.4
Intestine	1	3.7 ± 1.1	2.5 ± 0.4	2.4 ± 0.6	3.4 ± 1.0	3.8 ± 1.1	2.4 ± 0.8	3.5 ± 0.6	3.2 ± 0.7
	3	2.3 ± 0.8	1.8 ± 0.4	2.1 ± 0.4	2.2 ± 0.4	2.8 ± 0.8	1.9 ± 0.5	2.8 ± 0.5	2.5 ± 0.6
	7	0.8 ± 0.2	1.4 ± 0.3	1.7 ± 0.3	1.2 ± 0.3	1.5 ± 0.3	1.4 ± 0.4	1.3 ± 0.3	1.2 ± 0.3

*Values given as %ID/g tissue ± SD.
†Protein doses in the radiolabeled preparations were 50 μg each for ^{88}Y-cDTPA, ^{88}Y-DOTA, ^{88}Y-SCN-Bz-DTPA, and ^{186}Re-MAG3; 30 μg each for ^{177}Lu-cDTPA, ^{177}Lu-SCN-Bz-DTPA, and ^{177}Lu-DOTA; and 16 μg for ^{125}I.

Figures 5 and 6 show tumor growth curves of all individual mice, and Figure 7 shows the mean relative tumor growth per group. Individual mouse curves indicate that ^{90}Y-, ^{186}Re, and ^{177}Lu-labeled cG250 treatments initiated the longest median delays of exponential tumor growth (Table 5). Mice in the 3 control groups did not show a statistically significant difference in exponential tumor growth delay (overall mean, approximately 8 d). In subsequent statistical analysis, therefore, mice in the 3 control groups were pooled. Treatment with ^{177}Lu-SCN-Bz-DTPA-cG250 resulted in the longest delay in tumor growth (approximately 200 d). This was significantly longer than the delays observed with ^{90}Y-SCN-Bz-DTPA-cG250 ($P = 0.016$) and ^{186}Re-MAG3-cG250 ($P < 0.001$). The ^{90}Y-labeled cG250 group did not differ significantly ($P = 0.38$) from the ^{186}Re-labeled cG250 group in tumor growth delay (125 and 90 d, respectively). These 2 groups differed significantly ($P < 0.001$) from the group treated with ^{131}I-cG250 (tumor growth delay of 27 d), which again differed significantly from the control groups ($P < 0.001$).

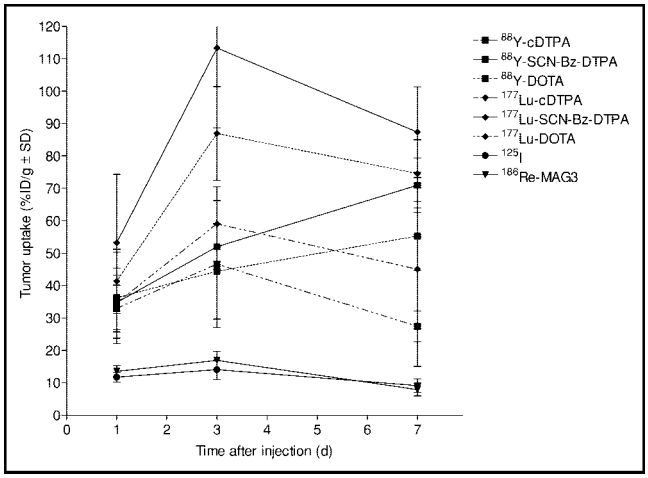

FIGURE 3. Biodistribution results of uptake in tumor of ^{88}Y- and ^{177}Lu-labeled cDTPA, SCN-Bz-DTPA, and DOTA-cG250; ^{125}I-cG250; and ^{186}Re-MAG3-cG250 at 1, 3, and 7 d after injection.

DISCUSSION

To directly compare the therapeutic efficacy of the cG250 antibody labeled with ^{131}I, ^{90}Y, ^{177}Lu, or ^{186}Re, we first determined the most suitable chelate and conjugation procedure for labeling the antibody with $^{88/90}$Y or ^{177}Lu. The in vitro stability of DOTA was slightly better than that of SCN-Bz-DTPA, with the difference between the 2 conju-

TABLE 4
Calculated Mean Absorbed Dose in Tumors at Maximum Tolerated Dose (MTD)

Radioimmunoconjugate preparation	Self-dose S value* (mGy/MBq · s)	AUC (h)	Absorbed tumor dose (Gy)
^{131}I-cG250	1.305	29.16	76
^{186}Re-MAG3-cG250	1.9215	16.30	104
^{90}Y-SCN-Bz-DTPA-cG250	2.055	46.17	95
^{177}Lu-SCN-Bz-DTPA-cG250	1.2035	201.44	807

*For tumors of 0.055 g (MIRDOSE3, unit density sphere model) (*24*).
AUC = area under the curve.

gates becoming apparent only after >14 d incubation. However, in our study the higher stability of the DOTA-chelated radiometallic mAbs resulted in a significantly lower femur uptake compared with SCN-Bz-DTPA–chelated cG250 at 7 d after injection. This is in agreement with the results of Camera et al. (*26*), who reported virtually no release of ^{88}Y from p-nitrobenzyl-DOTA (2B-DOTA) (0.5% ± 0.06%), whereas only a 5% release of activity was noted for 2 DTPA-derivative chelates 2-(p-SCN-Bz)-cyclohexyl-DTPA (A isomer) and 2-(p-SCN-Bz)-6-methyl-DTPA after 17 d of incubation in serum. Nevertheless, in vivo this resulted in a significantly higher cortical bone uptake for the DTPA-derivative chelates than for DOTA (2.8 ± 0.2 %ID/g and 3.0 ± 0.3 %ID/g versus 1.2 ± 0.1 %ID/g at 7 d after injection, respectively) (*26*). Govindan et al. (*27*) reported a more marked difference in the in vitro stability of ^{90}Y-DOTA and ^{90}Y-Bz-DTPA, with a 0.4% versus 10.7% respective dissociation after 11 d incubation in serum. This also resulted in similar tumor and tissue uptake in nude mice bearing human B-cell lymphoma xenografts over a 10-d period, with the exception of bone uptake, which was up to 50% lower for ^{88}Y-DOTA-hLL2 than for ^{88}Y-Bz-DTPA-hLL2 (*27*). Whether DOTA is also superior for ^{177}Lu has not been shown conclusively. Stein et al. (*28*) used DOTA as the chelate for facile and stable radiolabeling of mAb RS7 with ^{177}Lu and ^{88}Y and observed nearly identical biodistribution results for the radionuclides as did we when using DOTA as the chelate. On the other hand, Milenic et al. (*10*) performed a comparison of the performance of the SCN-Bz-DTPA and DOTA ligands as chelates to radiolabel mAb CC49 with ^{177}Lu. In biodistribution studies, these researchers observed no apparent significant differences between the conjugates tested, suggesting similar stabilities. Based on improved labeling efficiency and immunoreactivity, they prefered SCN-Bz-DTPA as the chelate for radiolabeling mAbs with ^{177}Lu for RIT applications (*10*). The biodistributions of ^{177}Lu-SCN-Bz-DTPA-cG250 and ^{177}Lu-DOTA-cG250 observed in our study provide evidence that there might be a slight difference in in vivo stability between these 2 immunoconjugates, because uptake of ^{177}Lu-SCN-Bz-DTPA-cG250 was slightly higher in most tissues, including bone, and markedly higher in liver and spleen. However, we did not observe this phenomenon in the corresponding ^{88}Y-labeled cG250 groups, except for a slight difference in uptake in bone, and the in vitro stability did not show a difference between SCN-Bz-DTPA and DOTA when labeled with ^{88}Y or ^{177}Lu. Furthermore, the liver and spleen uptake of ^{177}Lu-SCN-Bz-DTPA-cG250 was unexpectedly higher than even ^{177}Lu-cDTPA-cG250. Therefore, we are cautious to draw conclusions about the in vivo stability of the ^{177}Lu-SCN-Bz-DTPA-cG250 group.

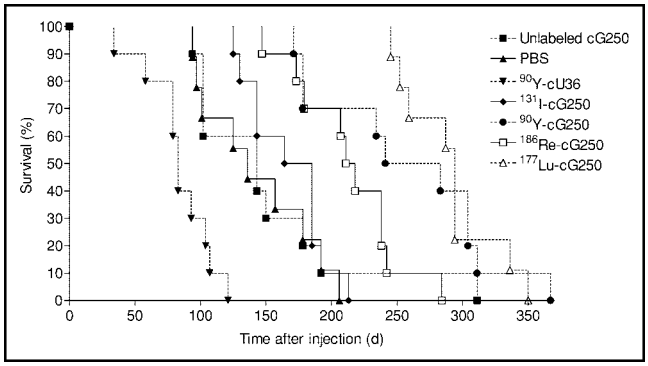

FIGURE 4. Survival curves of groups treated at MTD (^{131}I-cG250, ^{186}Re-MAG3-cG250, ^{90}Y-ITC-Bz-DTPA-cG250, and ^{177}Lu-ITC-Bz-DTPA-cG250 groups), and controls (unlabeled cG250, PBS, and 5.6 MBq [150 mCi] ^{90}Y-cU36 groups).

We used the same considerations as Milenic et al. (*10*) when we proceeded with the immunoconjugate SCN-Bz-DTPA-cG250 for RIT of RCC. Because higher specific activities could be obtained with the SCN-Bz-DTPA-cG250 conjugate, we used this immunoconjugate for subsequent RIT experiments in nude mice with subcutaneous RCC tumors. When labeling DOTA conjugates with ^{90}Y or ^{177}Lu, traces of metal ions competing for complexation with DOTA apparently limit the maximum specific activity that can be obtained. So far, the requirement of a high specific activity (>10 mCi/mg) could be met only when derivatized DTPA was used as a chelate.

RIT studies in nude mice with subcutaneous RCC xenografts demonstrated that the therapeutic efficacy of cG250 labeled with ^{177}Lu or ^{90}Y was superior to that of ^{131}I-cG250. This is in line with our observations in the biodistribution studies: Tumor uptake with these residualizing radionu-

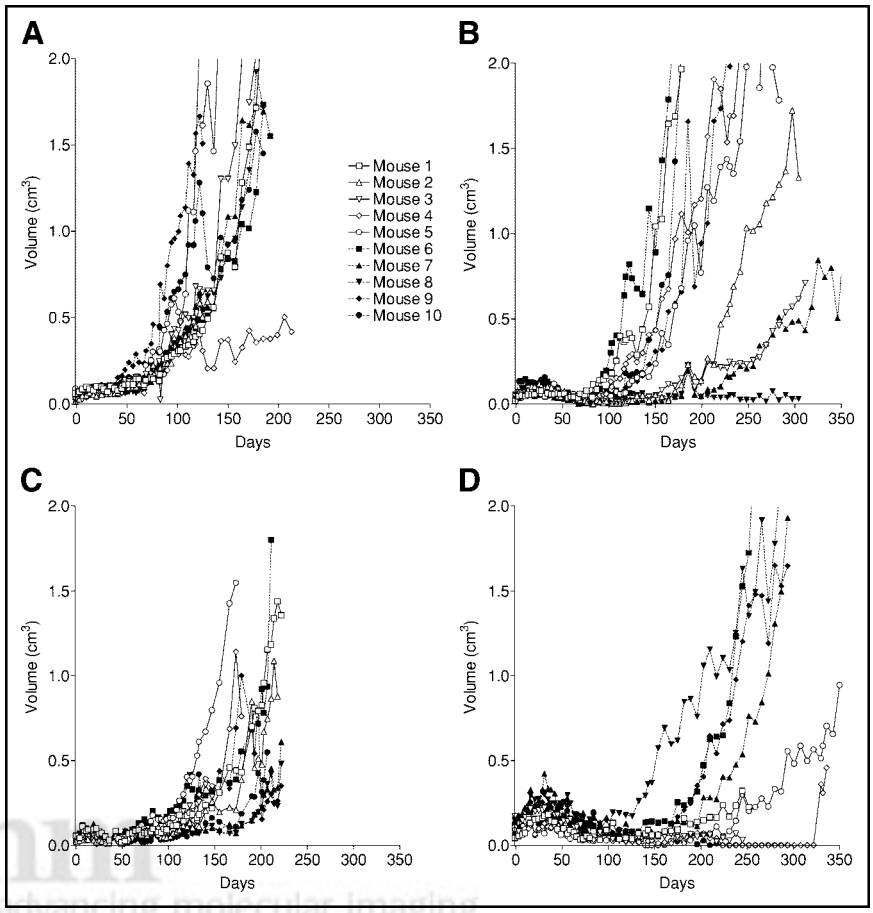

FIGURE 5. Tumor volume over time in groups treated with ^{131}I-cG250 (A), ^{90}Y-ITC-Bz-DTPA-cG250 (B), ^{186}Re-MAG3-cG250 (C), and ^{177}Lu-ITC-Bz-DTPA-cG250 (D).

clides was approximately 4 times higher than tumor uptake obtained with radioiodinated cG250. Numerous studies have demonstrated that the enhanced uptake of radionuclides such as ^{111}In and ^{90}Y is the result of intracellular retention of the radiolabeled catabolites after internalization of the radiolabeled antibody (*29–32*). In contrast, the lysosomal degradation product of radioiodinated mAbs, ^{131}I-tyrosine, is released from the target cell (*29,31*). As a result of the longer retention time of residualizing radionuclides in the tumor, higher radiation doses to the tumor are achieved, leading to an enhanced antitumor effect (*29,33,34*). Various radioiodination methods have now been developed that improve the intracellular retention of the iodine label in the target cell (*29,31,32,35,36)*). It might be worthwhile to consider these methods for labeling cG250 with ^{131}I. However, the physical disadvantages of ^{131}I, including relatively long half-life and high-energy γ-photons, would still remain.

The intracellular effect of a ^{186}Re-MAG3–labeled mAb on cell binding and internalization still needs to be elucidated. According to our observations in the biodistribution experiments, ^{186}Re-MAG3-cG250 showed a pattern nearly identical to that of ^{131}I-cG250, resulting in low tumor accretion and more rapid washout of the radiolabeled antibody preparation from the tumor (maximum tumor uptake, 17 %ID/g at 3 d after injection), which is similar to earlier results (*21,37*). Nevertheless, the results of the RIT experiments did show a difference in these 2 preparations. Although ^{131}I-cG250 showed a significantly shorter delay in tumor growth compared with ^{90}Y- and ^{177}Lu-labeled cG250, ^{186}Re-MAG3-cG250 performed as well as ^{90}Y-SCN-Bz-DTPA-cG250 (no significant difference) and significantly outperformed ^{131}I-cG250. This is in line with the results of Kievit et al. (*37*), who reported similar biodistribution results for ^{186}Re- and ^{131}I-labeled mAb 323/A3 that resulted in a 1.3-fold higher cumulative absorbed radiation dose in the tumor for ^{186}Re-labeled-323/A3. When mice were treated with equivalent radionuclide doses, tumor growth inhibition was also slightly better for the group injected with ^{186}Re-labeled 323/A3 (*37*). Because in our RIT experiments the MTD of ^{186}Re-cG250 was considerably higher than that of ^{131}I-cG250, this might explain the observed pronounced differences in tumor growth delay between mice treated with ^{186}Re-labeled and radioiodinated cG250.

Comparison of the RIT results of the current study with data from published literature on similar RIT experiments in nude mice is difficult, because experimental settings may differ widely (e.g., different sizes of tumor volume treated or various methods to dose the radiolabeled mAb). Second, the doses used for RIT can be based on established MTDs,

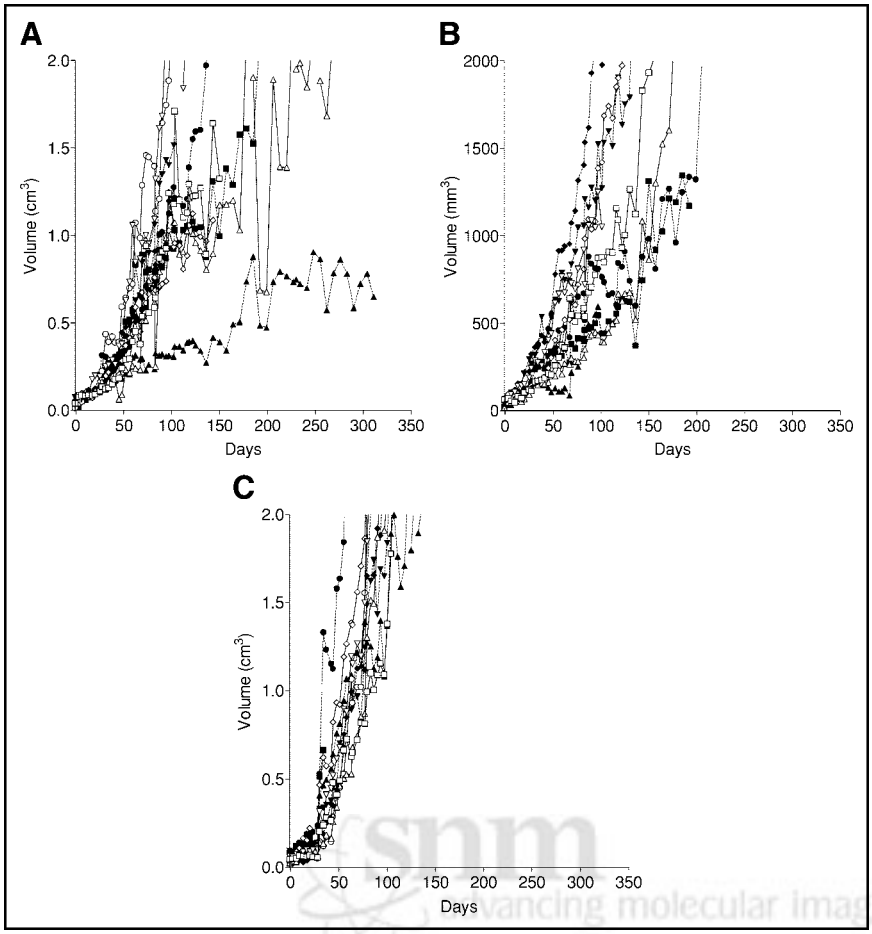

FIGURE 6. Tumor volume over time in control groups, including those treated with unlabeled cG250 (A), PBS (B), and 5.6 MBq (150 mCi) ^{90}Y-cU36 (C).

equivalent radionuclide doses, or even doses adjusted to deliver equal cumulative absorbed radiation doses to the tumor (*28*,*34*,*37*,*38*).

Although dosimetric calculations to estimate the absorbed radiation dose in the tumors can be fairly inaccurate as a result of the inaccuracy of the models used, the relative observed delays in tumor growth in the treatment groups (^{177}Lu was longer than ^{90}Y, which was approximately equal to ^{186}Re, which was longer than ^{131}I) corresponded to the respective calculated estimates of radiation-absorbed dose in the tumors (^{177}Lu was greater than ^{186}Re, which was greater than ^{90}Y, which was greater than ^{131}I).

The fact that the residualizing radionuclides ^{90}Y and ^{177}Lu when labeled to mAbs performed much better than conventionally radiolabeled mAbs has also been demonstrated previously (*33*,*34*). However, unlike Stein et al. (*28*), who

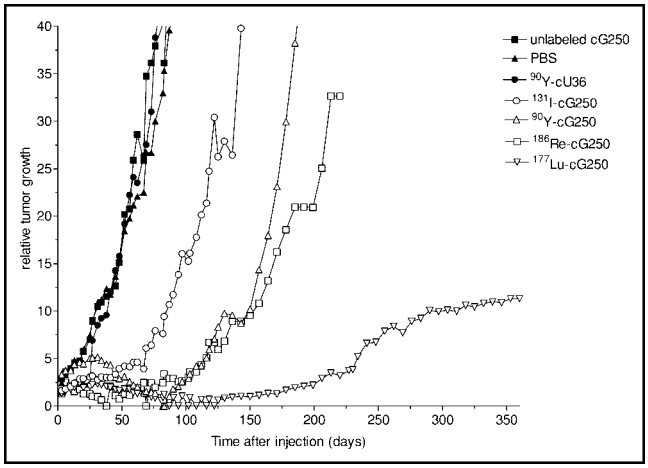

FIGURE 7. Mean relative tumor growth in time for all groups (^{131}I-cG250, ^{90}Y-ITC-Bz-DTPA-cG250, ^{186}Re-MAG3-cG250, ^{177}Lu-ITC-Bz-DTPA-cG250, unlabeled cG250, PBS, and ^{90}Y-cU36).

TABLE 5
Calculated Mean Delay in Exponential Tumor Growth for RIT and Control Groups

Radioimmunoconjugate preparation	Mean exponential tumor growth delay (d ± SD)
Unlabeled cG250	7.9 ± 4.1
PBS	6.0 ± 5.0
^{90}Y-SCN-Bz-DTPA-cU36	9.6 ± 4.4
^{131}I-cG250	26.6 ± 10.2
^{90}Y-SCN-Bz-DTPA	124.5 ± 69.1
^{186}Re-MAG3	90.0 ± 30.5
^{177}Lu-SCN-Bz-DTPA	186.4 ± 34.7

did not find a marked difference in biodistribution and therapeutic efficacy between ^{90}Y- and ^{177}Lu-labeled mAb RS7 in a direct comparison, our RIT experiments showed that ^{177}Lu-SCN-Bz-DTPA-cG250 was superior even to ^{90}Y-SCN-Bz-DTPA-cG250. This could be explained in part by the small size of the tumors used in the current experiments when compared with the large, established tumors (mean tumor volume, 0.85 cm^3) in the RIT experiments performed by Stein et al. (*28*). The smaller size of the tumor volumes would be to the advantage of ^{177}Lu as compared with ^{90}Y, the former being the β-emitter with the lowest energy and, therefore, better suited to irradiate small tumors. Siegel et al. (*39*) and O'Donoghue et al. (*40*) calculated that in small tumors a relatively large portion of the emitted energy of ^{90}Y is deposited outside the tumor, compared with radionuclides with a lower-energy β-emission, such as ^{131}I or ^{177}Lu. Recently, De Jong et al. (*3*) showed that ^{90}Y-DOTA-TYR$_3$-octreotide was able to induce tumor regression in rats, especially in tumors of medium size (3–9 cm^3). However, in small tumors (<1 cm^3), this effect was less pronounced. In contrast, the growth of small tumors (<1 cm^3) could be prevented effectively with an identical radiation dose (60 Gy) to the tumor with ^{177}Lu-DOTA-TYR$_3$-octreotate, nicely providing experimental evidence for this theory (*38*). In addition, the half-life of ^{177}Lu is better suited for the relatively slow pharmacokinetics of radiolabeled whole-IgG antibody. Blood clearance and tumor uptake of radiolabeled cG250 are slow, and thus a higher tumor dose is obtained with ^{177}Lu than with ^{90}Y.

We recently demonstrated that cG250 labeled with residualizing radionuclides had a higher uptake in RCC lesions in humans than does conventionally radioiodinated cG250 (*41*). Depending on the size of the lesions at which treatment is aimed (macroscopic metastases, microscopic or small-volume disease, or in an adjuvant setting), RIT with cG250 labeled with ^{90}Y or ^{177}Lu may have an impact in patients with RCC.

CONCLUSION

These experimental RIT studies clearly showed that the therapeutic efficacies of the cG250 preparations labeled with ^{177}Lu, ^{90}Y and ^{186}Re are superior to that of ^{131}I-cG250. ^{177}Lu showed the best antitumor effect, most likely as a result of optimal radiation characteristics for small tumors and a physical half-life that better matches mAb pharmacokinetics. The present study shows that especially the residualizing radionuclides ^{90}Y and ^{177}Lu are potentially better candidates for RIT studies in patients with RCC than is conventionally radiolabeled ^{131}I using mAb cG250.

ACKNOWLEDGMENTS

Ton Feuth, Department of Epidemiology and Biostatistics, University Medical Center (UMC) Nijmegen, is gratefully acknowledged for his advice on statistical analysis. Wil Buijs, PhD (Department of Nuclear Medicine, UMC Nijmegen), performed the dosimetric calculations. The authors thank Gerry Grutters, Bianca Lemmers, and Hennie Eikholt of the Central Animal Laboratory, UMC Nijmegen, for excellent technical assistance. The Dutch Cancer Society supported this work through grant number KUN99-1973. Egbert Oosterwijk, PhD, is supported by the Ludwig Institute for Cancer Research, New York, NY.

REFERENCES

1. Steffens MG, Boerman OC, Oosterwijk-Wakka JC, et al. Targeting of renal cell carcinoma with iodine-131-labeled chimeric monoclonal antibody G250. *J Clin Oncol.* 1997;15:1529–1537.
2. Steffens MG, Boerman OC, De Mulder PH, et al. Phase I radioimmunotherapy of metastatic renal cell carcinoma with ^{131}I-labeled chimeric monoclonal antibody G250. *Clin Cancer Res.* 1999;5(suppl):3268S–3274S.
3. De Jong M, Breeman WA, Bernard BF, et al. Tumor response after [(90)Y-DOTA(0), TYR(3)]octreotide radionuclide therapy in a transplantable rat tumor model is dependent on tumor size. *J Nucl Med.* 2001;42:1841–1846.
4. Muller WA, Schaffer EH, Linzner U. Studies on incorporated short-lived beta-emitters with regard to the induction of late effects. *Radiat Environ Biophys.* 1980;18:1–11.
5. Sharkey RM, Kaltovich FA, Shih LB, et al. Radioimmunotherapy of human colonic cancer xenografts with ^{90}Y labeled monoclonal antibodies to carcinoembryonic antigen. *Cancer Res.* 1988;48:3270–3275.
6. Hnatowich DJ, Childs RL, Lanteigne D, et al. The preparation of DTPA-coupled antibodies radiolabeled with metallic radionuclides: an improved method. *J Immunol Methods.* 1983;65:147–157.
7. Roselli M, Schlom J, Gansow OA, et al. Comparative biodistributions of yttrium- and indium-labeled monoclonal antibody B72.3 in athymic mice bearing human colon carcinoma xenografts. *J Nucl Med.* 1989;30:672–682.
8. Kozak RW, Raubitschek A, Mirzadeh S, et al. Nature of the bifunctional chelating agent used for radioimmunotherapy with yttrium-90 monoclonal antibodies: critical factors in determining in vivo survival and organ toxicity. *Cancer Res.* 1989;49:2639–2644.
9. Harrison A, Walker CA, Parker D, et al. The in vivo release of ^{90}Y from cyclic and acyclic ligand-antibody conjugates. *Int J Rad Appl Instrum B.* 1991;18:469–476.
10. Milenic DE, Garmestani K, Chappell LL, et al. In vivo comparison of macrocyclic and acyclic ligands for radiolabeling of monoclonal antibodies with ^{177}Lu for radioimmunotherapeutic applications. *Nucl Med Biol.* 2002;29:431–442.
11. Griffiths GL, Goldenberg DM, Knapp FF Jr, et al. Direct radiolabeling of monoclonal antibodies with generator-produced rhenium-188 for radioimmunotherapy: labeling and animal biodistribution studies. *Cancer Res.* 1991;51:4594–4602.
12. Visser GW, Gerretsen M, Herscheid JD, et al. Labeling of monoclonal antibodies with rhenium-186 using the MAG3 chelate for radioimmunotherapy of cancer: a technical protocol. *J Nucl Med.* 1993;34:1953–1963.
13. Fritzberg AR, Abrams PG, Beaumier PL, et al. Specific and stable labeling of antibodies with technetium-99m with a diamide dithiolate chelating agent. *Proc Natl Acad Sci USA.* 1988;85:4025–4029.
14. Oosterwijk E, Ruiter DJ, Hoedemaeker PJ, et al. Monoclonal antibody G250 recognizes a determinant present in renal-cell carcinoma and absent from normal kidney. *Int J Cancer.* 1986;38:489–494.
15. Velders MP, Litvinov SV, Warnaar SO, et al. New chimeric anti-pancarcinoma monoclonal antibody with superior cytotoxicity-mediating potency. *Cancer Res.* 1994;54:1753–1759.
16. Grabmaier K, Vissers JL, De Weijert MC, et al. Molecular cloning and immunogenicity of renal cell carcinoma-associated antigen G250. *Int J Cancer.* 2000;85:865–870.
17. Uemura H, Nakagawa Y, Yoshida K, et al. MN/CA IX/G250 as a potential target for immunotherapy of renal cell carcinomas. *Br J Cancer.* 1999;81:741–746.
18. Pastorekova S, Parkkila S, Parkkila AK, et al. Carbonic anhydrase IX, MN/CA IX: analysis of stomach complementary DNA sequence and expression in human and rat alimentary tracts. *Gastroenterology.* 1997;112:398–408.
19. Ruegg CL, Anderson-Berg WT, Brechbiel MW, et al. Improved in vivo stability and tumor targeting of bismuth-labeled antibody. *Cancer Res.* 1990;50:4221–4226.
20. Lewis MR, Raubitschek A, Shively JE. A facile, water-soluble method for modification of proteins with DOTA. Use of elevated temperature and optimized pH to achieve high specific activity and high chelate stability in radiolabeled immunoconjugates. *Bioconjug Chem.* 1994;5:565–576.

21. Steffens MG, Kranenborg MH, Boerman OC, et al. Tumor retention of ^{186}Re-MAG3, ^{111}In-DTPA and ^{125}I labeled monoclonal antibody G250 in nude mice with renal cell carcinoma xenografts. *Cancer Biother Radiopharm.* 1998;13:133–139.
22. Lindmo T, Boven E, Cuttitta F, et al. Determination of the immunoreactive fraction of radiolabeled monoclonal antibodies by linear extrapolation to binding at infinite antigen excess. *J Immunol Methods.* 1984;72:77–89.
23. Ebert T, Bander NH, Finstad CL, et al. Establishment and characterization of human renal cancer and normal kidney cell lines. *Cancer Res.* 1990;50:5531–5536.
24. Stabin MG. MIRDOSE personal computer software for internal dose assessment in nuclear medicine. *J Nucl Med.* 1996;37:538–546.
25. Schrijvers AH, Quak JJ, Uyterlinde AM, et al. MAb U36, a novel monoclonal antibody successful in immunotargeting of squamous cell carcinoma of the head and neck. *Cancer Res.* 1993;53:4383–4390.
26. Camera L, Kinuya S, Garmestani K, et al. Evaluation of the serum stability and in vivo biodistribution of CHX- DTPA and other ligands for yttrium labeling of monoclonal antibodies. *J Nucl Med.* 1994;35:882–889.
27. Govindan SV, Shih LB, Goldenberg DM, et al. ^{90}Yttrium-labeled complementarity-determining region-grafted monoclonal antibodies for radioimmunotherapy: radiolabeling and animal biodistribution studies. *Bioconjug Chem.* 1998;9:773–782.
28. Stein R, Govindan SV, Chen S, et al. Radioimmunotherapy of a human lung cancer xenograft with monoclonal antibody RS7: evaluation of ^{177}Lu and comparison of its efficacy with that of ^{90}Y and residualizing ^{131}I. *J Nucl Med.* 2001;42:967–974.
29. Shih LB, Thorpe SR, Griffiths GL, et al. The processing and fate of antibodies and their radiolabels bound to the surface of tumor cells in vitro: a comparison of nine radiolabels. *J Nucl Med.* 1994;35:899–908.
30. Press OW, Shan D, Howell-Clark J, et al. Comparative metabolism and retention of iodine-125, yttrium-90, and indium-111 radioimmunoconjugates by cancer cells. *Cancer Res.* 1996;56:2123–2129.
31. Geissler F, Anderson SK, Venkatesan P, et al. Intracellular catabolism of radiolabeled anti-mu antibodies by malignant B-cells. *Cancer Res.* 1992;52:2907–2915.
32. Sharkey RM, Behr TM, Mattes MJ, et al. Advantage of residualizing radiolabels for an internalizing antibody against the B-cell lymphoma antigen, CD22. *Cancer Immunol Immunother.* 1997;44:179–188.
33. Stein R, Juweid M, Mattes MJ, et al. Carcinoembryonic antigen as a target for radioimmunotherapy of human medullary thyroid carcinoma: antibody processing, targeting, and experimental therapy with ^{131}I and ^{90}Y labeled mAbs. *Cancer Biother Radiopharm.* 1999;14:37–47.
34. Stein R, Chen S, Haim S, et al. Advantage of yttrium-90-labeled over iodine-131-labeled monoclonal antibodies in the treatment of a human lung carcinoma xenograft. *Cancer.* 1997;80(suppl):2636–2641.
35. Stein R, Goldenberg DM, Thorpe SR, et al. Effects of radiolabeling monoclonal antibodies with a residualizing iodine radiolabel on the accretion of radioisotope in tumors. *Cancer Res.* 1995;55:3132–3139.
36. Stein R, Govindan SV, Mattes MJ, et al. Improved iodine radiolabels for monoclonal antibody therapy. *Cancer Res.* 2003;63:111–118.
37. Kievit E, van Gog FB, Schlüper HMM, et al. Comparison of the biodistribution and efficacy of monoclonal antibody 323/A3 labeled with either 131-I or 186-Re in human ovarian cancer xenografts. *Int J Radiat Oncol Biol Phys.* 1997;38:813–823.
38. De Jong M, Breeman WA, Bernard HF, et al. Receptor-targeted radionuclide therapy using radiolabelled somatostatin analogues: tumour size versus curability [abstract]. *Eur J Nucl Med.* 2001;28:1026.
39. Siegel JA, Stabin MG. Absorbed fractions for electrons and beta particles in spheres of various sizes. *J Nucl Med.* 1994;35:152–156.
40. O'Donoghue JA, Bardies M, Wheldon TE. Relationships between tumor size and curability for uniformly targeted therapy with beta-emitting radionuclides. *J Nucl Med.* 1995;36:1902–1909.
41. Brouwers AH, Buijs WCAM, Oosterwijk E, et al. Targeting of metastatic renal cell carcinoma with the chimeric monoclonal antibody G250 labeled with ^{131}I or ^{111}In: an intrapatient comparison. *Clin Cancer Res.* 2003;9(suppl):3953S–3960S.